Publications of the Astronomical Society of Australia

An international journal of astronomy and astrophysics

www.publish.csiro.au/journals/pasa

Molecular Hydrogen in the Lagoon: H$_2$ Line Emission from Messier 8

Michael G. Burton[1,2]

[1]School of Physics, University of New South Wales, Sydney, NSW 2052, Australia
[2]School of Cosmic Physics, Dublin Institute for Advanced Studies, 5 Merrion Square, Dublin 2, Ireland
M.Burton@unsw.edu.au

Abstract: The 2.12 µm v = 1–0 S(1) line of molecular hydrogen has been imaged in the Hourglass region of M8. The line is emitted from a roughly bipolar region, centred around the O7 star Herschel 36. The peak H$_2$ 1–0 S(1) line intensity is 8.2×10^{-15} erg s^{-1} cm^{-2} arcsec^{-2}. The line centre emission velocity varies from -25 km s^{-1} in the SE lobe to $+45$ km s^{-1} in the NW lobe. The distribution is similar to that of the CO J = 3–2 line. The H$_2$ line appears to be shock-excited when a bipolar outflow from Herschel 36 interacts with the ambient molecular cloud. The total luminosity of all H$_2$ lines is estimated to be $\sim$16 L$_\odot$ and the mass of the hot molecular gas $\sim 9 \times 10^{-4}$ M$_\odot$ (without any correction for extinction).

Keywords: infrared: ISM — H$_{II}$ regions — ISM: individual (M8) — ISM: molecules — molecular processes — shock waves — stars: formation

1 Introduction

The Lagoon Nebula, Messier 8 (also known as NGC 6523), is an H$_{II}$ region located behind NGC 6530. M8 is embedded within a molecular cloud which extends to the young ($\sim 2 \times 10^6$ years old) star cluster that is NGC 6530, centred $10'$ to its east (Lada et al. 1976). Star formation is presumed to have proceeded from NGC 6530 and is now active in M8. Within M8's core lies the O7v star Herschel 36 (Woolf 1961), which has created a blister-type H$_{II}$ region, the Hourglass. This visually distinctive nebula is extended $15''$EW and $30''$NS, and lies $15''$E of Herschel 36. The Hourglass is embedded within a larger H$_{II}$ region, $\sim 3'$ across, also ionised by Herschel 36. These lie within an extended H$_{II}$ region, $\sim 0.5°$ across, ionised by two O stars, HD 165052 and 9 Sgr (Woolf 1961; Lada et al. 1976). Near Herschel 36 are a number of obscured sources, first observed in the near-IR by Allen (1986). Woodward et al. (1990) have designated them KS1 to KS5. Together, they may form a cluster of hot stars, analogous to the Trapezium in the Orion Nebula (M42), where θ^1_c Ori is the dominant member. In the mid-IR *MSX*[1] sky survey, this region appears as bright, extended source, with a 21 µm continuum flux of 960 Jy. This source is also prominent in the sub-mm and mm continuum (Tothill 1999; Richter, Stecklum, & Launhardt 1998). Near Herschel 36, narrow band optical imaging with the *HST* reveals an object reminiscent of the proplyds in the Orion Nebula — a star within a bow-shock arc, whose apex is pointed towards Herschel 36 (Stecklum et al. 1998). It is presumed to be an externally ionised circumstellar disk. These authors also estimate the distance to M8 to be 1.8 kpc, based on the association with NGC 6530.

Of particular interest to this paper are the observations by White et al. (1997) of intense CO line emission from M8. They found the peak CO J = 3–2 intensity to be over 100 K, making it the second brightest CO line source known. The CO J = 3–2 and 4–3 lines were mapped and found to have a loose, bipolar structure, extending NW–SE from Herschel 36. Taking the broad CO line profiles (extending over 20 km s^{-1}), and the presence of a jet-like object extending 0.5$''$SE of Herschel 36 in *HST* images (Stecklum et al. 1995), it seems likely that there is a molecular outflow in the core of M8. If so, it would be expected for there to be molecular hydrogen line emission as well, both shocked (from the deceleration of the outflow by the ambient cloud) and fluorescent (excited by far-UV photons from Herschel 36). However, White et al. (1997) also searched for the near-IR H$_2$ v = 1–0 S(1) line in M8, but did not detect it. In this paper we report more sensitive observations for H$_2$ emission from M8, and find that there is indeed excited H$_2$ line emission from this source.

2 Observations and Data Reduction

The Hourglass region of the Lagoon Nebula was imaged on 1997, July 22, using the IRIS 1–2.5 µm camera, in conjunction with the University of New South Wales Infrared Fabry-Pérot etalon (UNSWIRF, Ryder et al. 1998), on the 3.9 m Anglo Australian Telescope (AAT). The UNSWIRF etalon has a FWHM spectral resolution of $\sim$75 km s^{-1}, a pixel size of 0.77$''$, and a 100$''$ circular field of view. It is scanned through a spectral line of interest in order to obtain an emission line image of a source, with minimal contamination from any continuum radiation present. It also permits limited kinematic information to be obtained, through the emission velocity of the line centre across the field of view.

The H$_2$ 1–0 S(1) (2.1218 µm) line was observed. Following a rapid scan to determine the plate spacing for the line centre, three on-line plate spacings were used

---

[1] See http://irsa.ipac.caltech.edu/ for details.

for imaging, spaced by 39 km s⁻¹, together with an off-line setting, 840 km s⁻¹ to the blue. Integration times were two minutes per plate spacing, and in addition, a sky frame, 300″N, was obtained immediately after each source frame.

The star BS 6748 ($K = 4.57$ mag) served as the flux standard, and was imaged at each etalon spacing. The absolute accuracy in flux calibration using a Fabry-Pérot etalon is around 30%. A diffused dome lamp provided a flat field for each etalon spacing. An arc lamp was scanned through a free spectral range in order to wavelength calibrate the etalon response for each pixel of the array.

Data reduction was undertaken using a custom software package using IRAF[2]. Frames are linearised, flat-fielded using a dome flat taken at the appropriate plate spacing, cleaned of bad pixels, and sky-subtracted. They are then shifted to align stars in each frame and smoothed with a Gaussian filter. The off-line frame is then subtracted from each on-line frame (having been appropriately scaled to minimise residuals from the subtraction process). The three on-line frames form a data cube comprised of two spatial and one spectral dimension. The spectral dimension is fitted, pixel-by-pixel, with the instrumental profile (a Lorentzian), to yield a line image. Finally, a coordinate frame was added, using the digitised sky survey[3] to relate common stars between the visible and 2.1 μm.

The line centre at each pixel position is obtained from the plate spacing determined for the peak of the fitted profile (i.e. the spacing which maximises the transmission of the H₂ line). Where the S/N is adequate the velocity can be determined to a precision of order 10 km s⁻¹. Absolute line emission velocities were determined with reference to the plate spacing found for the peak of the H₂ emission in M17. Relative plate spacings are then transformed to a velocity difference between M8 and M17, with the absolute velocity of the H₂ line in M17 taken to be +21 km s⁻¹ (V_{LSR}). Note that, as a consequence of the broad wings to the instrumental profile, the line width cannot be determined unless it is very much wider than the spectral resolution (which is not the case in M8).

3 Results

The field surrounding the Hourglass is shown in the 3-colour near-IR image in Figure 1. The J (1.25 μm), H (1.65 μm), and K (2.2 μm) images were previously obtained by the author and David Allen during the commissioning of IRIS in 1991. They have been combined to produce a 3-colour image which simulates the appearance of the nebula if our eyes were sensitive to the 1–2.5 μm wavelength range. Embedded and obscured stars are red or yellow and foreground stars are blue. The HII region of the Hourglass appears blue as its near-IR emission is dominated by Paschen lines of hydrogen in the J-band.
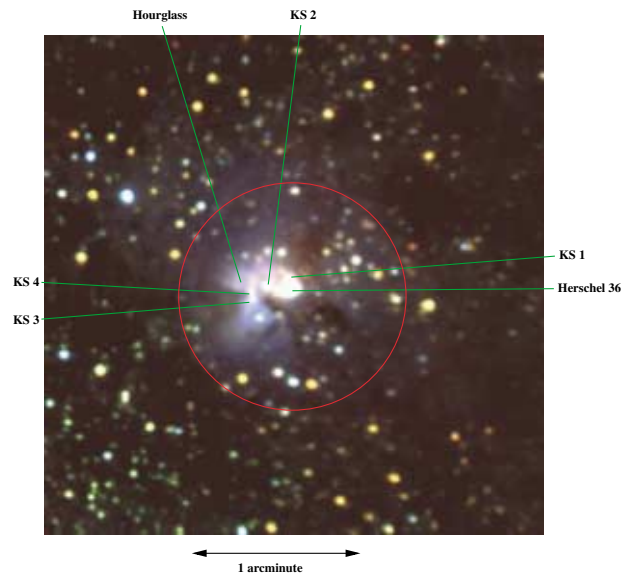
[2] Image Reduction and Analysis Facility (see http://iraf.noao.edu).
[3] See http://stdatu.stsci.edu/dss/

Figure 1 Three-colour near-infrared image of M8. Blue denotes the J (1.25 μm) band, green the H (1.65 μm) band, and red the K (2.2 μm) band. The field imaged with UNSWIRF is indicated by the red circle. Several features of interest are labelled: Herschel 36 (the O7V star powering the HII region emission), the near-IR sources KS1–KS4, and the Hourglass. Heavily reddened stars appear red or yellow and foreground stars blue. The Hourglass is blue because the near-IR emission is dominated by Paschen recombination lines of hydrogen in the J-band.
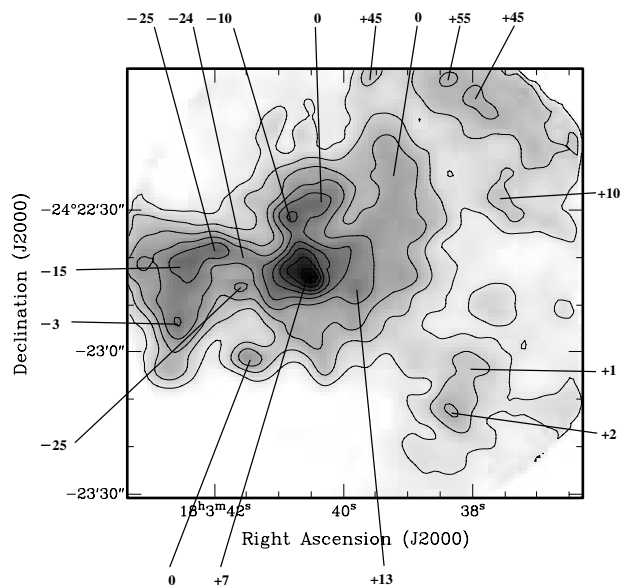

Figure 2 Image of the molecular hydrogen v = 1–0 S(1) line emission at 2.12 μm in M8, overlaid with contours of the line emission. Contours start at, and are in steps of, 8.5×10^{-16} erg s⁻¹ cm⁻² arcsec⁻². Also indicated are the H₂ line centre velocities, in km s⁻¹ (V_{LSR}), at selected locations.

The morphology of the Hourglass is the same in the three bands, suggesting that this is its intrinsic shape, rather than being determined by variable extinction in the optical (as suggested by Woodward et al. 1986). In the figure, Herschel 36 and the Hourglass are marked, as well as the four 2 μm sources KS1–KS4 (Woodward et al. 1990).

The molecular hydrogen v = 1–0 S(1) line emission image of M8 is shown in Figure 2, overlaid with contours of the line flux. The emission is clumped and the morphology broadly bipolar, centred about Hershel 36. Also shown are the line centre velocities for selected locations, obtained from fitting the instrumental profile to the three on-line images. While the accuracy of individual velocities is no better than $\sim 10\,\mathrm{km\,s^{-1}}$, they do indicate that there is a velocity gradient of $\sim 70\,\mathrm{km\,s^{-1}}$ across the field, extending from $\sim -25\,\mathrm{km\,s^{-1}}$ to the east of Herschel 36, to $\sim +45\,\mathrm{km\,s^{-1}}$ to its north-west.

The $2.12\,\mu\mathrm{m}$ H_2 line emission is compared to the $2.2\,\mu\mathrm{m}$ K-band continuum emission in Figure 3. It can be seen that the H_2 emission peaks close to the continuum peak at Herschel 36. The Hourglass, however, appears as a cavity in the H_2 distribution. H_2 line fluxes have been determined for the apertures indicated in this figure, and are listed in Tabl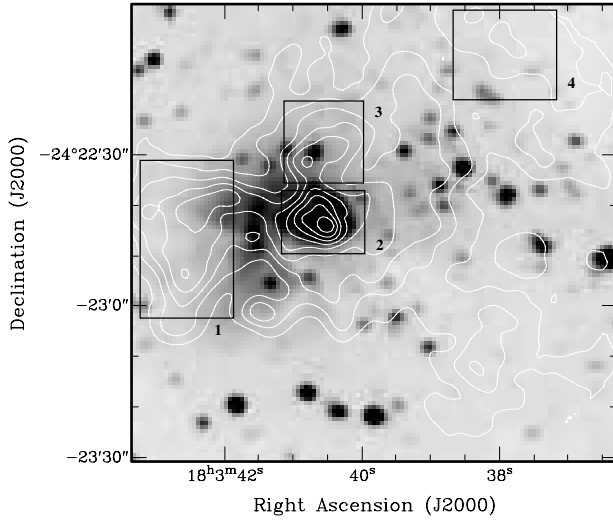e 1, together with the positions of the emission peaks. The total 1–0 S(1) line emission from the region is $1.0 \times 10^{-11}\,\mathrm{erg\,s^{-1}\,cm^{-2}}$ and the peak intensity is $8.2 \times 10^{-15}\,\mathrm{erg\,s^{-1}\,cm^{-2}\,arcsec^{-2}}$. At an assumed distance of 1.8 kpc for M8, these figures are equivalent to a luminosity in the 1–0 S(1) line of $1.1\,\mathrm{L_\odot}$, and to a peak column density in the $(v,J) = (1,3)$ level of the H_2 molecule of $1.4 \times 10^{16}\,\mathrm{cm^{-2}}$ (without any correction applied for extinction to the emitting region).

An enlarged image of the H_2 line emission, overlaid on the K-band continuum, is shown in Figure 4. It is apparent that the H_2 emission does not, in fact, peak at the location of Herschel 36. The H_2 emission peaks approximately $(1.5''\mathrm{E}, 0.5''\mathrm{S})$ from Herschel 36, roughly halfway between it and the proplyd $(2.5''\mathrm{E}, 1.5''\mathrm{S})$ of Herschel 36.

Figure 3 Image of the K-band ($2.2\,\mu\mathrm{m}$) continuum emission from M8, overlaid with contours of the H_2 1–0 S(1) $2.12\,\mu\mathrm{m}$ line emission. Contours are as in Figure 2. The numbered boxes refer to the apertures in Table 1.
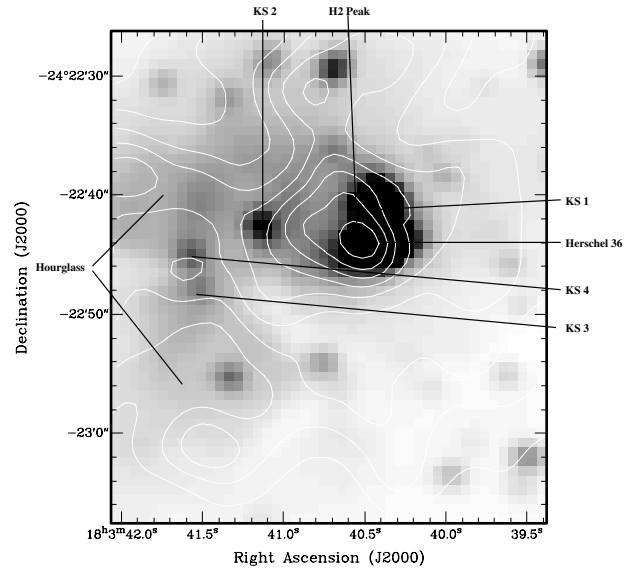

Figure 4 Enlarged image of the central region of M8, showing the K-band continuum, overlaid by contours of the H_2 1–0 S(1) line emission. Contour levels are as in Figures 2 and 3. The separation between the H_2 peak and Herschel 36, the exciting star for the Hourglass, is apparent. These features are labelled, together with the infrared sources KS1–KS4.

Table 1. Molecular hydrogen line fluxes in M8

Region[1]	RA[2] 18^h03^m	Dec[2] $-24°22'$	Aperture[3] (arcsec)	1–0 S(1) Flux[4] $\times$ $10^{-13}\,\mathrm{erg\,s^{-1}\,cm^{-2}}$	1–0 S(1) Peak intensity[5] $\times$ $10^{-15}\,\mathrm{erg\,s^{-1}\,cm^{-2}\,arcsec^{-2}}$
1	42.5^s	$22''$	22×32	17.6 ± 0.1	4.8 ± 0.5
2	40.5^s	$44''$	17×13	11.1 ± 0.1	8.2 ± 0.5
3	40.8^s	$31''$	17×17	9.2 ± 0.1	5.3 ± 0.5
4	38.4^s	$02''$	20×22	7.8 ± 0.1	2.7 ± 0.5
Total[6]	40.5^s	$44''$	89×79	102 ± 3	8.2 ± 0.5

[1] Aperture, as shown in Figure 3.
[2] Position of peak emission within the aperture, in J2000.
[3] Size of aperture.
[4] Total H_2 1–0 S(1) line emission from aperture.
[5] Peak emission intensity within aperture.
[6] Integrated fluxes for the entire field.

4 Discussion

4.1 H$_2$ Morphology and Kinematics

Given the intensity of the CO line emission measured in M8 by White et al. (1997), it was a considerable surprise when the same authors failed to detect any H$_2$ line emission from the source. M8 is the second most intense CO source detected, and clearly a site of active massive star formation. White et al. imaged M8 through a narrow band (1% width) filter centred on the H$_2$ 1–0 S(1) line, and used a broad band 2.2 μm image to subtract the continuum from it. They failed to detect any H$_2$ line emission, and placed an upper limit of $\leq 3.4 \times 10^{-4}$ erg s^{-1} cm^{-2} sr^{-1} on the line flux. This is equivalent to $\leq 8 \times 10^{-15}$ erg s^{-1} cm^{-2} arcsec^{-2}, equal to the peak intensity we actually measured in M8. Thus, the upper limit of White et al. (1997) is consistent with our detection of H$_2$ line emission. It does, however, highlight the difficulty of measuring line emission through narrow band filters in the presence of a strong continuum, and the advantages of using a Fabry-Pérot etalon for such measurements. The 1σ detection limit we achieved, with just 6 minutes on-line integration, is 3×10^{-16} erg s^{-1} cm^{-2} arcsec^{-2}.

Comparison with the ^{12}CO J = 3–2 image obtained by White et al. (1997) (see their Figure 2a, within the outermost white contour, at a level of 230 K km s^{-1}) shows that the morphology is very similar to the H$_2$ 1–0 S(1) line, given the difference in resolution of the two images (the CO 3–2 image was obtained through a 14″ beam). The line emission is peaked around Herschel 36, and extends in two lobes in a NW–SE direction, ∼45″ from the centre. There is a minimum in the CO emission around the Hourglass, as there is with the H$_2$ emission. The extension to the SW is also seen in both line images. This corresponds to a region of increased extinction seen in optical images.

The CO 3–2 line also displays broad line profiles, extending from +2 to +22 km s^{-1} (V$_{LSR}$), and peaking at +10 km s^{-1} near Herschel 36. Profiles in the NW lobe tend to extend somewhat further to the red than they do in the SE lobe. Similar behaviour is displayed by the H$_2$ line centre velocities, though the velocity extent is considerably larger than for the CO line. The H$_2$ velocity ranges from ∼ −25 km s^{-1} in the SE lobe, to +7 km s^{-1} at the emission peak, to ∼ +45 km s^{-1} in the NW lobe.

4.2 Shock Excitation

High spatial resolution imaging in the optical lines of Hα and [SII] with the *HST*, and with adaptive optics in the K and L band near-IR continuum (Stecklum et al. 1995), shows an ionised, jet-like feature, extending ∼0.5″ from Herschel 36 to the SE (the K and L band emission is presumed to be dominated by the 2.16 μm Brγ and 4.05 μm Brα hydrogen recombination lines). Taken with the morphology and velocity extent of both the CO and H$_2$ line emission, this suggests that the H$_2$ line is shock-excited. It would appear to be the result of an interaction of a wind or jet from Herschel 36 with the ambient molecular cloud.

The H$_2$ morphology then represents the location where a loosely collimated bipolar flow from Herschel 36, surrounding an ionised jet, runs into a molecular cloud. The larger velocities seen in H$_2$ than CO represent the shock speeds where the outflow impacts the molecular cloud. The flow then cools and decelerates, and this compressed gas is seen in the lower-velocity CO lines.

Presuming that the H$_2$ line emission is dominated by shocks, it is possible to estimate the total H$_2$ line luminosity and the mass of hot, post-shock gas. In molecular shocks, the total H$_2$ line luminosity is typically ∼15 times the 1–0 S(1) line flux, and the fraction of hot H$_2$ that is in the (v,J) = (1,3) state of the molecule is ∼2% (e.g. see Burton 1992). The total H$_2$ line luminosity from the source is then ∼16 L$_\odot$, and the peak column density of hot H$_2$ is 6.1×10^{17} cm^{-2} (i.e. at the emission peak). The total mass of hot H$_2$ in the source is ∼9 × 10^{-4} M$_\odot$. These figures should be corrected for an unknown amount of extinction to the emitting region. This cannot be obtained from our data, so we will use the estimates of A$_v$ ∼ 5 mag towards Herschel 36 and the proplyd, made by Stecklum et al. (1998). This is equivalent to ∼0.5 mag at 2.1 μm. If this is representative of the extinction to the H$_2$ emitting region, then the extinction-corrected luminosity, peak column density, and mass of hot H$_2$ are ∼25 L$_\odot$, ∼10^{18} cm^{-2}, and ∼1.5 × 10^{-3} M$_\odot$, respectively.

These figures can be compared to the total amount of molecular gas and its peak column density, estimated by White et al. (1997) from the CO lines. They determined these to be ∼31 M$_\odot$ and 1.3×10^{23} cm^{-2}, respectively. These values are very much greater than the quantities determined for the hot molecular gas, as expected if the hot material comprises just a thin skin of material in front of cooled, compressed gas. The cooling time for hot H$_2$, τ_{cool}, is ∼1 year, which therefore suggests that the outflow must have existed for ∼10^4−10^5 years.

The mechanical luminosity of the outflow can be estimated as

$$L_{mech} \sim 0.5 M_{hot} V^2 / \tau_{cool}, \qquad (1)$$

where M_{hot} is the mass of hot H$_2$ and V is the average speed of the shock wave. Taking this to be 35 km s^{-1} (half the range in velocity of the H$_2$ line emission) yields $L_{mech} \sim 300$ L$_\odot$ (extinction corrected), an order of magnitude greater than the H$_2$ line luminosity. This is obviously a crude estimate, but it does indicate that the H$_2$ lines are a significant contributor, and possibly the major one (given the assumptions made), to the cooling of the gas behind the shock front.

4.3 Fluorescence

Despite our conclusion that the H$_2$ line emission is dominated by shocks, there may still be a significant contribution by far-UV fluorescence to parts of it. The Hourglass is an H$_{II}$ region, excited by the UV radiation from Herschel 36. The gap in the H$_2$ emission around the Hourglass suggests a physical connection between the

two, for instance the Hourglass may be a cavity embedded within the outflow. The H_2 line velocity over the Hourglass is approximately constant, taking the value $\sim -25\,\mathrm{km\,s^{-1}}$ (V_{LSR}). A constant velocity would be expected for fluorescent emission from a molecular cloud with small internal motions (e.g. see Burton et al. 1990). The velocity measured then indicates the V_{LSR} velocity of the surface of the photodissociation region. This velocity, $-25\,\mathrm{km\,s^{-1}}$, is at the negative limit of the $50\,\mathrm{km\,s^{-1}}$ range for the ionised gas in the Hourglass, as measured through [OIII] 5007 Å line emission (Chakraborty & Anandarao 1999). Furthermore, Woodward et al. (1986) have detected 3.28 μm PAH emission from the region around the Hourglass. This is excited by the same far-UV photons that can fluorescently excite H_2 (e.g. see the PAH emission in NGC 6334; Burton et al. 2000). Therefore, it seems likely that some of the H_2 emission, especially in the vicinity of the Hourglass, is fluorescently excited. However, with our data, it is not possible to estimate what fraction this might be.

5 Conclusions

Strong near-IR molecular hydrogen line emission is produced from around the Hourglass in the M8 star forming region. The peak H_2 brightness is at the detection limit of a previous attempt to measure H_2 line emission from the source, thus explaining the reported non-detection. The H_2 is emitted from an extended, roughly bipolar region, centred on the powering source for the Hourglass, Herschel 36. It is orientated along a NW–SE direction. The morphology is similar to that of the CO J = 3–2 distribution in M8. Taken with the $\sim 70\,\mathrm{km\,s^{-1}}$ variation in the H_2 line centre across the region, and the $20\,\mathrm{km\,s^{-1}}$ width of the CO profiles, this suggests that the H_2 emission is shock-excited, when a bipolar outflow, originating from Herschel 36, impacts the surrounding molecular cloud. The total H_2 line luminosity is $\sim 16\,\mathrm{L_\odot}$ (not corrected for any extinction). The H_2 lines radiate a significant fraction of the mechanical energy deposited by the shocks, but we cannot yet determine whether H_2 line emission is the dominant coolant in the shocked gas.

To examine the excitation mechanism more closely, in particular to determine whether there may also be fluorescent H_2 emission, it would be necessary to measure higher excitation lines of the molecule, from v $\geq$ 2. This could be done either by long-slit spectroscopy, or through further Fabry-Pérot imaging, with the waveplates tuned to appropriate lines. To improve the determination of the flow energetics it will be necessary to use greater spectral resolution and resolve the line profiles, in order to measure the momentum and kinetic energy distribution of the hot molecular gas across the source.

References

Allen, D. A. 1986, MNRAS, 319, 35P

Burton, M. G. 1992, AuJPh, 45, 463

Burton, M. G., Geballe, T. R., Brand, P. W. J. L., & Moorhouse, A. 1990, ApJ, 352, 625

Burton, M. G., et al. 2000, ApJ, 542, 359

Chakraborty, A., & Anandarao, B. G. 1999, A&A, 346, 947

Lada, C. J., Gull, T. R., Gottlieb, C. A., & Gottlieb, E. W. 1976, ApJ, 203, 159

Richter, S., Stecklum, B., & Launhardt, R. 1998, Abstracts of contributed talks and posters presented at the annual scientific meeting of the Astronomische Gesellschaft, Heidelberg, September 14–19, 1998

Ryder, S. D., Allen, L. E., Burton, M. G., Ashley, M. C. B., & Storey, J. W. V. 1998, PASA, 15, 228

Stecklum, B., Henning, T., Eckart, A., Howell, R. R., & Hoare, M. 1995, ApJ, L153

Stecklum, B., Henning, T., Feldt, M., Hayward, T. L., Hoare, M. G., Hofner, P., & Richter, S. 1998, AJ, 115, 767

Tothill, N. F. H. 1999, PhD Thesis, Queen Mary and Westfield College, University of London

White, G. J., Tothill, N. F. H., Matthews, H. E., McCutcheon, W. H., Huldtgren, M., & McCaughrean, M. J. 1997, A&A, 323, 529

Woodward, C. E., Pipher, J. L., Helfer, H. L., & Forrest, W. J. 1990, ApJ, 365, 252

Woodward, C. E., et al. 1986, AJ, 91, 870

Woolf, N. J. 1961, PASP, 73, 206